



Contribution of coral composition to color red in the uniform color space CIE 1976L*a*b*

Yushu Yang^a, Ying Guo^{a,*}, Ye Zhang^b, Yanrong Zou^c, Jinyu Wei^d, Lu Liang^e

^aSchool of Gemmology, China University of Geosciences, Beijing 100083, China, email: guoying@cugb.edu.cn (Y. Guo)

^bDepartment of science and technology, Dehong Teachers' College, Mangshi 678400, China

^cSchool of Foreign Language, Shanghai Normal University, Shanghai 200234, China

^dSchool of Management, China University of Geosciences Great Wall College, Baoding 071000, China

^eMarketing Department, National Gemstone Testing Center, Beijing 100013, China

Received 30 October 2018; Accepted 27 January 2019

ABSTRACT

The paper is a study of the color appearance and chromogenic pigment of red coral, using spectrophotometer and Raman spectrometer. The results shows that under the standard D_{65} light source, the color of 86 pieces of coral samples is white-red with a hue angle $h_0 \in (21.07, 151.98)$; the lightness value is $L^* \in (32.97, 88.70)$, which is above average; the chroma value is $C^* \in (1.40, 48.42)$, with a large variation range. The chromogenic pigment in red coral is a mixture of two polyene pigments, both of which are cis-trans isomeric. One pigment is red with a hue angle h_0 of about 20 degrees and the other pigment is yellow-orange with a hue angle $h_0 > 50$ degrees. Red coral also contains some colorless and opaque substances, which affect the lightness L^* and transparency of coral. The results show that the content of these colorless and opaque substances is related to the species of coral. In the future, if the specimens are further enriched and a database is established, it will help to distinguish the species of coral without damage.

Keywords: Red coral composition; Red coral pigment; Raman spectrum; Uniform color space

1. Introduction

Red coral belongs to the family Coralliidae, whose skeletons have been known worldwide for their use as gemstones and ornaments [1–3]. Their common colors are white, yellow, pink, orange, orange-red, red and crimson. According to species and origins, the red corals on the market can be divided into *Corallium japonicum* [4], *Corallium konojoi* [4,5], *Corallium elatius* [6] and *Corallium secundum* [7] in the Pacific region, and *Corallium rubrum* [8–10] in the Mediterranean and North Atlantic [11] region.

The skeletons of red coral consist of inorganic and organic components [12–15], whose mineral component is calcium carbonate [12] crystallized in the form of calcite, and whose organic component accounts for less than 2% of the

total weight of the skeletons, including proteins, lipids and sugars [13].

The color origin of red and pink corals has not yet been fully explained until now [1,16–19]. In 1937, Ranson and Durivault [20] proposed that red coral was colored by red iron salt, which was later proved wrong. In 1992, Allemand and Grillo [21] studied the Raman spectrum characteristics of carotenoids and pointed out that carotenoids are common chromogenic pigments in animals in nature. In 1986, Merlin studied red coral by resonance Raman spectroscopy. Raman spectra showed characteristic spectral lines similar to those of carotenoid molecules. Compared with the Raman spectra of standard carotenoids, it was found that the stretching vibration signal of pigment C–C in red coral was shifted in the Raman spectra. Therefore he proposed two hypotheses for

* Corresponding author.

polyene pigments in red coral: carotenoids containing side methyl groups and polyacetylene chains without side methyl groups [12]. These two hypotheses have aroused a wide debate in academic circles.

In 2007, Cvejic and Tambutté et al. [33] successfully extracted canthaxanthin and its trans-structure from *Corallium rubrum*. However, they only mass spectrometry was used to prove the extracted components, so the argument that the extracted component was canthaxanthin was questioned by scholars, but the extraction process was confirmed [22,23]. The same period, a polyene pigment containing 8–16 conjugated C=C bonds is considered to be the organic chromogenic pigment of red coral [18,24,25]. Recently, Ain et al. [26] have applied density functional theory to analyze the structure and vibrational Raman spectra of the all-trans polyene model of *Corallium rubrum* in detail. It is concluded that the all-trans polyene pigment in *Corallium rubrum* contains 11–12 conjugated C=C bonds, and the larger the number of C=C and C–C polyenes contains, the stronger the corresponding Raman signal will be. Therefore, polyenes containing less conjugate bonds will generate weak signals, which will be covered by other polyenes containing more conjugated bonds. As a result, the Raman spectra cannot indicate that *Corallium rubrum* merely contains a single polyene pigment.

The perception and influencing factors of red coral color are light source, red coral and the observer. Different light sources have different spectral energy distribution and red coral itself selectively absorbs visible light, so that red coral presents different color characteristics.

Colorimetric system is increasingly used in gemmological research [27–30], such as tourmaline [31], jadeite [32–35], golden citrine [36], etc. CIE 1976 L*a*b* color space has good uniformity, suitable for the expression and calculation of all object colors. Accordingly, it is widely adopted and used by all countries in the world as an international common color measurement system [31]. Prior to this, no one has applied CIE chromaticity theory to quantitative description of red coral color, specifically quantifying the visual characteristics of color. Therefore, the paper combines Raman spectroscopy with CIE chromaticity theory to study the color appearance and chromogenic pigment of red coral.

2. Materials and methods

2.1. Samples

The 86 pieces of coral samples adopted in this experiment are all surface polishing, some of which are branches

of coral and the rest are corals with oval surface, belonging to three biological species and one unknown biological species, respectively (Table 1). The color of coral samples varies from white to crimson and from translucent to opaque with resin-glass luster. The measured part is uniform in color, with a minimum sample size of 5 × 8 mm and a maximum sample size of 68 × 79 mm. The spectrophotometer tests the spot diameter of 4 mm, and the Raman spectrometer can measure the spot microscopically, and the sizes of these samples meet the measurement requirements of both.

2.2. Experimental instruments

2.2.1. Raman spectrometer

In this experiment, 86 samples of red coral are tested by Microscopes Raman Spectrometer at the Laboratory of School of Gemology, China University of Geosciences (Beijing).

Test Instrument: Lab RAM HR Evolution Raman Spectrometer

Test method: Argon ion laser 532 nm laser, scanning spot 100 nm

Test range: 100–1,065 cm⁻¹, 200–3,800 cm⁻¹

2.2.2. ASHLEY X-Rite SP62 integrating spherical spectrophotometer

The color data of 86 coral specimens are tested under the D_{65} light source by using the ASHLEY X-Rite SP62 integrating spherical spectrophotometer, with the measurement range of 360–750 nm, the measurement time of less than 2.5 s, the wavelength interval of 10 nm, and the voltage of 240 V, the current of 50–60 Hz. In addition, the test condition is reflection, including specular reflection, data results obtained using CIE1976L*a*b* uniform color space.

3. Results and discussion

3.1. Raman spectrum study of red coral

3.1.1. Raman spectrum of red coral

Even under intense laser irradiation, the color of the deep red precious coral used in jewellery is very stable, and there are no color changes in 86 Raman spectroscopy tests.

As shown in Fig. 1, the Raman spectra of the white corals in the front row have three strong signals at 284, 715, and 1,088 cm⁻¹. There are three weak signals at 1,750; 1,019; and 1,438 cm⁻¹ and these six signals are Raman signals belonging

Table 1
Colors and species of 86 samples used in this experiment

Color	<i>Corallium rubrum</i>	<i>Corallium elatius</i>	<i>Corallium japonicum</i>	Unknown species
White	–	M1-M2	–	01–02
Pink	–	M3-M11	–	03–08
Orange	–	M12-M18	–	09–11
Orange red	S1-S4	M19-M22	–	12–13
Red	S5-S16	M23-M28	A1-A17	–
Crimson	S17-S20	–	A18-A25	–

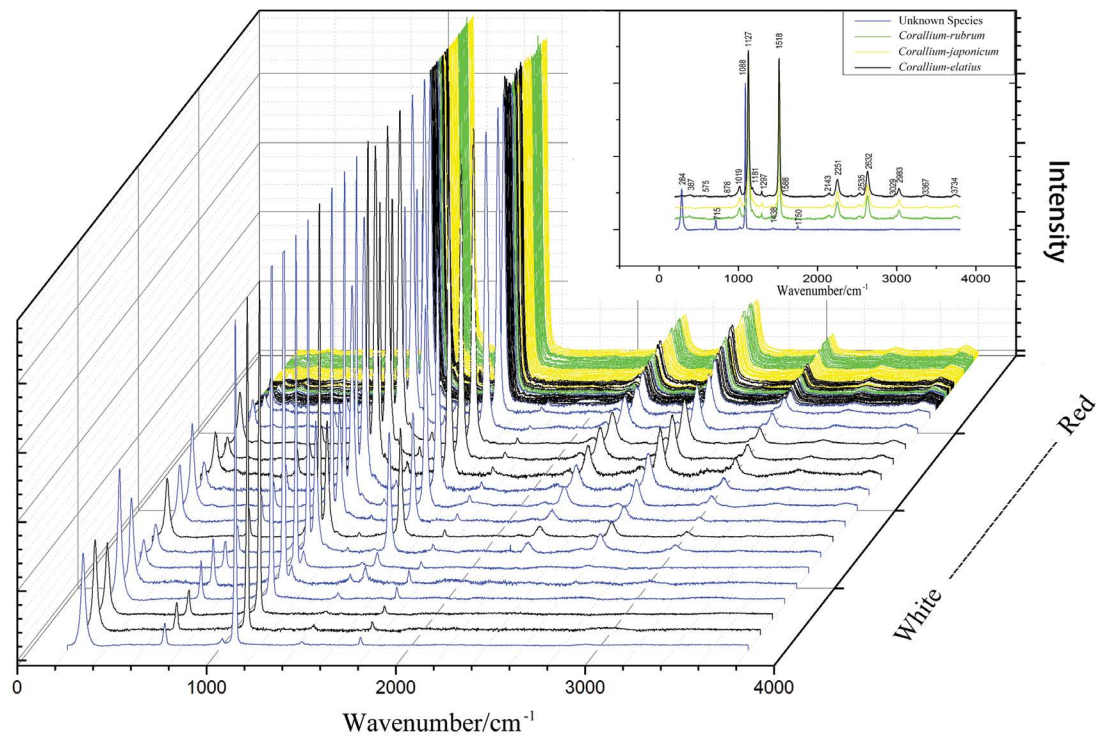


Fig. 1. Raman spectrum of 86 red coral samples.

Note: The Raman spectra of different species of corals are represented by different colors; the Raman spectra are arranged by appearance of the sample color, with white in front and red in the back; for convenient comparison, the Raman spectrum is pulled along the longitudinal axis.

Table 2
Red coral Raman shift spectrum signal position and its attribution

Wavenumbers (cm ⁻¹)	Calcite	Attribution	References
284	284	Calcite, rotational lattice mode	[37]
387	–	Organic	This work
575	–	Organic	This work
715	715	Calcite, CO ₃ in plane bending	[37]
878	–	Organic	This work
1,019	1,019	HCO ₃ ⁻ or CH ₃ rocking	[37]
1,088	1,088	Calcite, CO ₃ sym stretch	[37]
1,127	–	Organic, ν ₂ (C–C)	[12]
1,181	–	Organic	This work
1,297	–	Organic	This work
1,438	1,438	Calcite, CO ₃ sym stretch	[37]
1,518	–	Organic, ν ₁ (C=C)	[12]
1,588	–	Organic	This work
1,750	1,750	Calcite	[37]
2,143	–	Organic overtone/combinational	[37]
2,251	–	Organic, 2ν ₂	[37]
2,535	–	Organic overtone/combinational	[37]
2,632	–	Organic, ν ₁ + ν ₂	[37]
2,983	–	Organic overtone/combinational	[37]
3,029	–	Organic, 2ν ₁	[12]
3,367	–	Organic, 3ν ₂	[12]
3,734	–	Organic overtone/combinational	[37]

to calcite (Table 2) [12,37]. With the transition from white to red, that is, with the appearance of pigments and the increase of pigment concentration, there are six strong signals which are in 1,127; 1,181; 1,518; 2,251; 2,632; and 3,029 cm^{-1} in the Raman spectra of corals appearing and 10 weak signals at 387; 575; 878; 1,297; 1,588; 2,143; 2,535; 2,983; 3,367; and 3,734 cm^{-1} appearing. These 16 Raman signals belong to organic pigments (Table 2) [12,37]. As seen from the front to the back in Fig. 1, as the pigment content increases, the Raman signal of the organic pigment constantly gets stronger than that of the calcite, and the Raman signal of the calcite is weakened relative to the Raman signal of the pigment [38–48]. The signal at 1,019 cm^{-1} gets relatively stronger as the pigment concentration increases, and it belongs to both calcite and organic pigment.

As shown in Fig. 1, in the white and red coral samples, six signals belonging to calcite can be observed but no signal belonging to aragonite was observed. Once again, for the coral samples used in this paper, its inorganic composition is calcite crystals. The Raman spectral line of the coral shows that the Raman signal $\nu(284 \text{ cm}^{-1})$ produced by the rotation of the calcite lattice and the relative strength of the Raman signal $\nu(1,088 \text{ cm}^{-1})$ generated by the extension of the CO_3 system in the calcite will change. The same sample (S1) was tested by Raman spectroscopy from different directions and found that the relative strength change of this signal is because the angle between the laser direction and the direction of formation of the measured coral sample is different, which indicates that the coral is a calcite aggregate gemstone, and the calcite crystals inside the coral have the orientation in certain degree during aggregation. Comparing the Raman spectra of different species of corals, it is found that there is no significant difference in their Raman spectral signals, meaning that the coloring pigments are extremely likely to be the same. The pigmentation of pearls is a mixed polyene pigment [18], in comparison, the composition of such polyene pigments in red corals is probably not a single one, but is a mixture of 2–3 polyene pigments.

This organic pigment possesses two distinct strong Raman signals of 1,127 and 1,518 cm^{-1} and is a typical olefin containing conjugated C–C and C=C units. The vibration signal of C–C in carotenoids is about at 1,150 cm^{-1} , and the vibration signal of C–C in this organic pigment is located at 1,127 cm^{-1} which is a big difference. The change in the position of the C–C signal is due to a decrease in the number of CH_3 substituted on both sides of the all-trans polyene, which is considered to be not a carotenoid olefin. The Raman signal of the organic pigment at 1,019 cm^{-1} belongs to CH_3 , and the existence form of CH_3 has three possibilities:

- Exist at both ends of the organic dye polyene chain, and the substitution group at both ends of the organic dye polyene chain contains CH_3 ;
- Exist on both sides of the organic pigment polyene chain, that is, on both sides of the organic pigment – the amount of CH_3 is less than the carotenoid but not null;
- Exist on both sides of the organic pigment polyene chain and also on both ends of the organic color polyene chain. These three possibilities are all there to be further explored by future scholars.

3.1.2. Study on Raman spectrum signal intensity of organic pigments in red coral

Signal intensity is the area of the peak in Raman spectrum. The signal intensity at a certain position in Raman spectrum is related to the type of functional groups that generate signals, the energy intensity of laser excitation, and the number of functional groups (functional group concentration) per unit volume. After baseline treatment of the original Raman spectrum without longitudinal stretching, the peak fitting is performed to calculate the area and the signal intensity values at each position are obtained.

In Fig. 2, $\nu(1,127 \text{ cm}^{-1})$ signal strength is taken as the abscissa, signal strength of $\nu(1,019 \text{ cm}^{-1})$, $\nu(1,181 \text{ cm}^{-1})$, $\nu(1,518 \text{ cm}^{-1})$, $\nu(2,251 \text{ cm}^{-1})$, $\nu(2,632 \text{ cm}^{-1})$, and $\nu(3,027 \text{ cm}^{-1})$ are, respectively, taken as the input points in the ordinate coordinate, and input points of 86 pieces of red coral samples are concentrated in one figure. It can be seen that their signal strengths are basically positively correlated, but the correlation degree is slightly different. Use Origin to judge their correlation:

- The Pearson correlation coefficient of $\nu(1,127 \text{ cm}^{-1})$ and $\nu(1,019 \text{ cm}^{-1})$ is 0.97838;
- The Pearson correlation coefficient of $\nu(1,127 \text{ cm}^{-1})$ and $\nu(1,181 \text{ cm}^{-1})$ is 0.97108;
- The Pearson correlation coefficient of $\nu(1,127 \text{ cm}^{-1})$ and $\nu(1,518 \text{ cm}^{-1})$ is 0.99746;
- The Pearson correlation coefficient of $\nu(1,127 \text{ cm}^{-1})$ and $\nu(2,251 \text{ cm}^{-1})$ is 0.96488;
- The Pearson correlation coefficient of $\nu(1,127 \text{ cm}^{-1})$ and $\nu(2,632 \text{ cm}^{-1})$ is 0.96803;
- The Pearson correlation coefficient of $\nu(1,127 \text{ cm}^{-1})$ and $\nu(3,027 \text{ cm}^{-1})$ is 0.96101;
- Their correlation coefficients are all above 0.95.
- Therefore, the concentration of functional groups that generate these signals is positively correlated.

The signal $\nu(1,019 \text{ cm}^{-1})$ belongs to CH_3 , signal $\nu(2,251 \text{ cm}^{-1})$, $\nu(1,127 \text{ cm}^{-1})$ belongs to the C–C, signal $\nu(1,518 \text{ cm}^{-1})$,

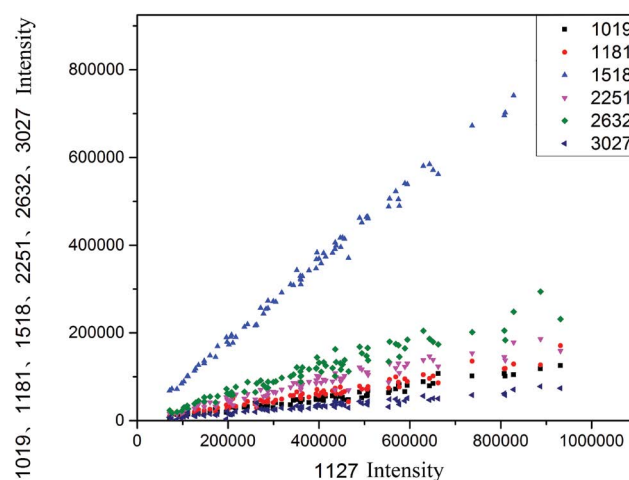


Fig. 2. Signal intensity projection of 86 pieces of red coral samples in the Raman spectra.

$\nu(3,027\text{ cm}^{-1})$ belongs to the C=C, $\nu(2,632\text{ cm}^{-1})$ belongs to the synergism of C–C and C=C, $\nu(1,181\text{ cm}^{-1})$. Its belonging is not clear (Table 2) [12,37]. It can be inferred that the concentration of CH₃, C–C, and C=C in organic pigments is positively correlated. This provides a basis for further analysis of the composition of organic pigments in red coral.

3.2. Study on red coral color based on CIE1976L*a*b* uniform color space

3.2.1. Coral color

Under the standard D_{65} light source, the color of 86 pieces of coral samples is white-red with a hue angle $h_0 \in (21.07, 151.98)$; the lightness value is $L^* \in (32.97, 88.70)$, which is above average; the chroma value is $C^* \in (1.40, 48.42)$, with a large variation range, which is consistent with the color appearance of the samples.

In addition to five samples with white appearance, tones of 81 samples are in the orange-red region with a hue angle $h_0 \in (21.07, 51.23)$, as shown in Fig. 3.

3.2.2. Pigment concentration of coral

The signal intensity of the Raman spectrum is positively correlated with the measured substance concentration.

The higher the concentration is, the stronger the signal will be, but the signal intensity is also affected by the tested laser energy, environment, noise, sample fluorescence, etc., so it is not viable to use the peak signal of organic matter with different corals to represent and then compare them.

The main component of red coral is calcite, which accounts for more than 98% of the total composition. Therefore, if the content of calcite in coral can be regarded as a relatively constant value, that is, the content of calcite in each coral sample is the same, Raman spectrum of will be the same too. Thus, the ratio of the signal intensity representing the organic pigment content and the signal intensity representing the calcite content is the relative content of the organic pigment in each sample, which is the concentration and recorded as Y .

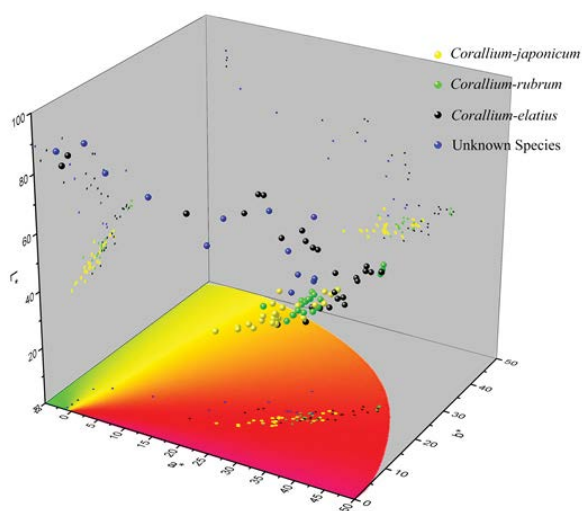


Fig. 3. Projection of 86 pieces of red coral samples in CIE 1976 L*a*b* uniform color space.

$\nu(1,088\text{ cm}^{-1})$ and $\nu(1,127\text{ cm}^{-1})$ are the strongest peaks of inorganic matter and the strongest signals of organic pigments, respectively, which are close. When the pigment concentration is small, the signal intensity of the two can be obtained relatively accurately; however, when the pigment concentration is large, the $\nu(1,088\text{ cm}^{-1})$ signal will be swallowed by the $\nu(1,127\text{ cm}^{-1})$ signal, and the error will be large.

$\nu(715\text{ cm}^{-1})$ and $\nu(1,019\text{ cm}^{-1})$, the signal intensity is positively correlated with $\nu(1,088\text{ cm}^{-1})$ and $\nu(1,127\text{ cm}^{-1})$ when the pigment concentration is large, and if the Raman measurement range is set at $100\text{--}1,065\text{ cm}^{-1}$, it is not affected by the signals of $\nu(1,088\text{ cm}^{-1})$ and $\nu(1,127\text{ cm}^{-1})$, but since the signal strength of $\nu(715\text{ cm}^{-1})$ is very weak, the error still exists.

In summary, the Y value needs to be considered simultaneously with the signal intensity ratios of $\nu(1,019\text{ cm}^{-1})$ and $\nu(715\text{ cm}^{-1})$, $\nu(1,127\text{ cm}^{-1})$ and $\nu(1,088\text{ cm}^{-1})$ in order to reduce the error, but when the pigment concentration is large, the error is still large. Therefore, in the factual study, it is necessary to utilize the Raman spectrum figure longitudinally stretched by samples of different samples to compare the relative intensity relationship between the inorganic signal and the organic pigment signal.

3.2.3. Relationship between coral pigment concentration and color

As shown in Fig. 4, the pigment concentration of red coral is negatively correlated with the lightness of red coral color, that is, the greater the pigment concentration is, the smaller the lightness L^* will be, and the color of red coral is the color of inorganic calcite and colorless and opaque organic matter, which is presented as white and has the high lightness. With the appearance of the pigment, the color appearance gradually changes to yellow, pink, orange, and orange red, and the lightness decreases, the pigment concentration further increases, and the color appearance color changes to red and deep red (Bovine blood), the brightness further decreases.

The points in Fig. 4 are dispersed because of different types of corals, calculation errors of pigment concentration, and systematic errors in experimental measurements. There is a large error in the calculation of the pigment concentration, but the pigment concentration and the brightness are significantly correlated. Therefore, in the study of the color of the red coral below, the lightness Y is used instead of the pigment concentration Y .

As shown in Fig. 5, when L^* value is higher and the range is from 55 to 90 (55, 90) and the pigment concentration is lower, the hue angle h_0 of the coral is still in the range of (23.98, 51.23), and the color of the coral changes from orange to red. As the pigment concentration increases, the brightness L^* decreases, and the value of h_0 becomes convergent, approaching $h_0 = 32$.

At low pigment concentration, the hue angle range is large, so the coloring pigment of the coral presenting the corals is not single, which are different colors. Among them, at least one red pigment exists, and orange-yellow pigment is also present, and changes of their ratios and concentration cause that when the coral is at a low pigment concentration, the changing range of h_0 is still large. In the pale yellow (04)

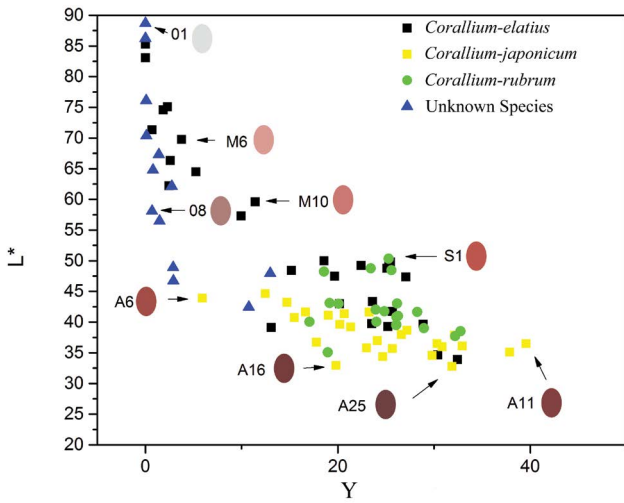


Fig. 4. Pigment concentration of red coral Y and color lightness of red coral.

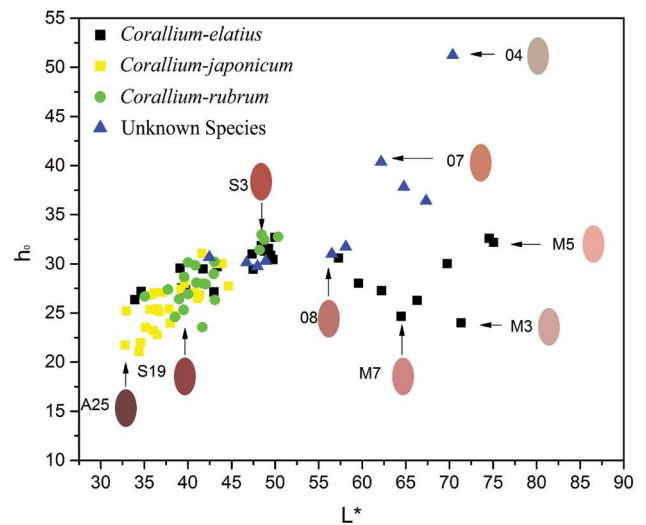


Fig. 5. Color lightness L^* and color hue angle h_0 of 81 red corals. Note: Color appearances of five corals are white and coral samples without organic pigment are not considered.

or pale pink (M3) samples, their organic pigment signals both appear on the Raman spectrum and both of orange and red are common colors of olefin pigments, which can be inferred that the two color pigments are olefins.

In 2018, Rozuki et al. [22] extracted two pigments from red corals by chromatography and found the same molecular weight by mass spectrometry; Ain et al. [26] applied density function theory to the study of red coral pigments, which shows that the pigment in red coral may not be single, but a mixture; their polyene chain length difference is within 2 and 3 C=C unit. The analysis of signal intensity of Raman spectrum from above shows that CH_2 , C–C, C=C are present in the mixed pigment and their numbers are positively correlated. We can make the assumption that the polyene pigment in the coral is not a single one, but is mixed by two polyene pigments. The two pigments are cis-trans

isomerism, and the length of the polyene chain and the type and number of functional groups are the same. The pigment produces red, the hue angle h_0 is about 20 degrees, and the other pigment produces yellow-orange, whose hue angle $h_0 > 50$ degrees. When L^* is low, whose range is (30, 55), the pigment concentration is high. As the pigment increases, L^* continues to decrease, and the hue angle h_0 of the coral color decreases from orange red to red. At high pigment concentrations, the decrease in hue angle h_0 may be due to an increase in the proportion of red pigment, or it may be because the red color of the red pigment masks the color of the yellow-orange pigment.

As shown in Fig. 6, different species of red coral have different hue angle h_0 and chroma C^* . Analyzed by origin, the Elson correlation coefficient between *Corallium japonicum*,

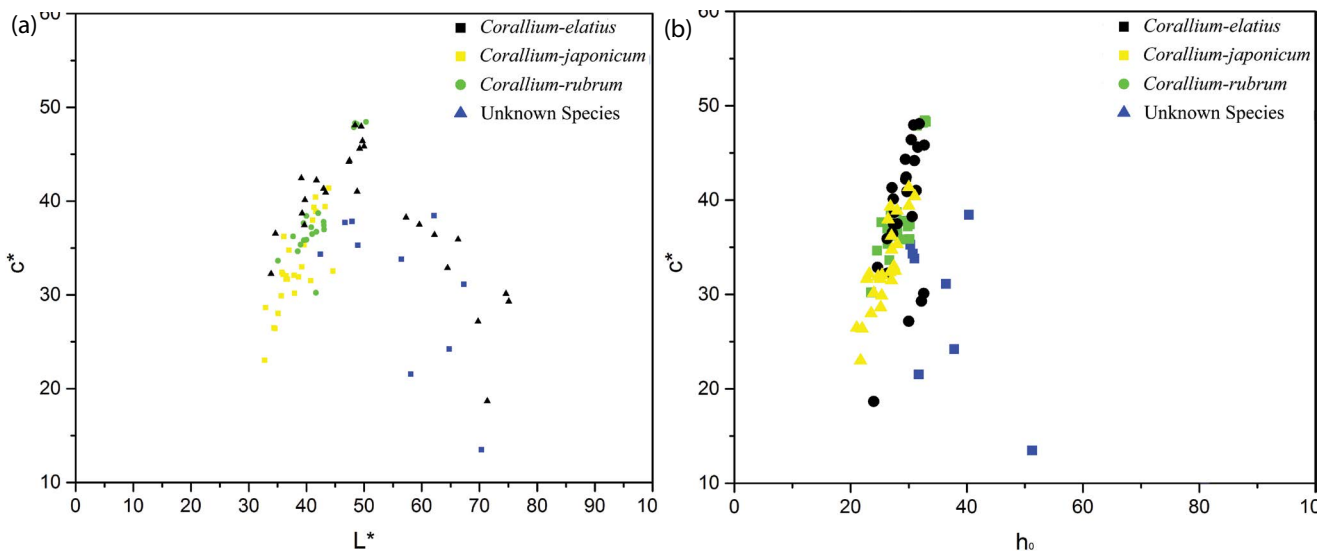


Fig. 6. (a) L^* and C^* of 81 red corals and (b) h_0 and C^* of 81 red corals.

Note: Color appearances of five corals are white and coral samples without organic pigment are not considered.

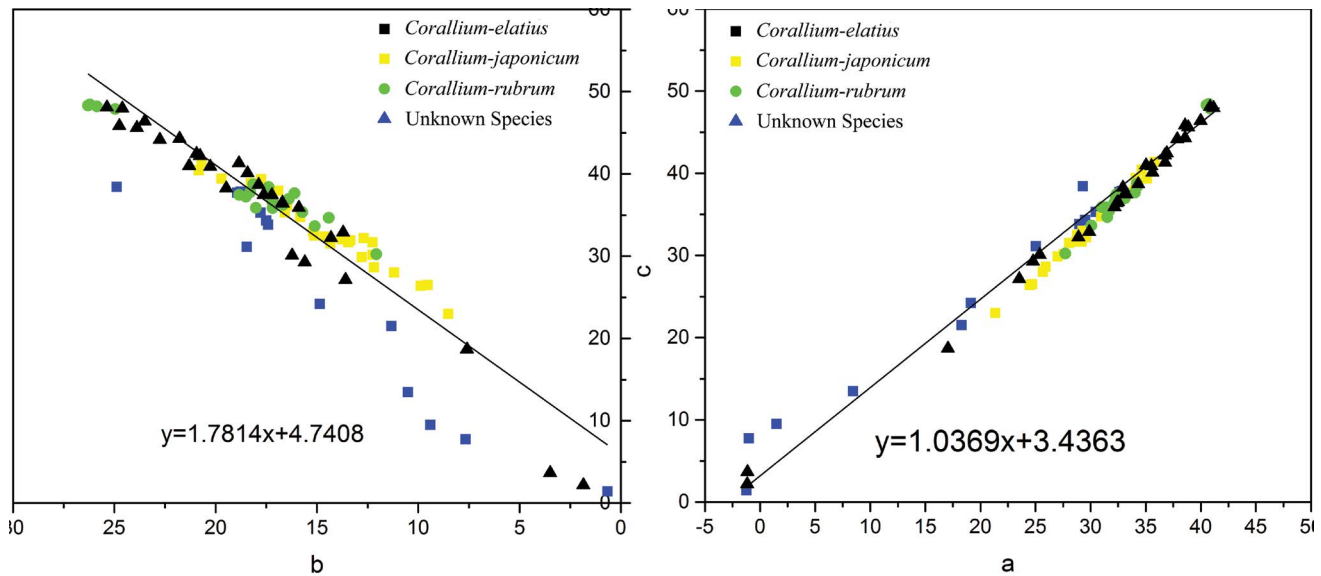


Fig. 7. Relationship between red coral's chroma C^* and a^* , b^* .

Corallium elatius, *Corallium rubrum* and unknown species, and red coral hue angle h_0 with chroma C^* is 0.86, 0.83, 0.84, and 0.23, respectively.

And the hue angle h_0 of *Corallium japonicum*, *Corallium elatius*, and *Corallium rubrum* is positively correlated with chroma C^* . The greater the hue angle is, the brighter the color will be. As shown in Fig. 6, when L^* is higher and the range is (55, 90), the pigment concentration is relatively lower and as the pigment concentration increases, L^* decreases and the color chroma C^* increases. When L^* is lower, the range is (30, 55), the pigment concentration is high, and as the pigment concentration increases, L^* decreases, and the color saturation C^* decreases. The pigments are from nothing to more, the color is from nothing to bright, the pigment concentration reaches a certain level and then rises, the color changes from bright to deep, and this process is also the process of increasing color chroma C^* and then decreasing.

As shown in Fig. 7, the chroma coefficient of red coral color C^* and a^* is 1.04, and the correlation coefficient with b^* is 1.78. The correlation coefficient between C^* and a^* is closer to 1, which indicates that relationship between a^* and b^* is closer and that red color contributes more than yellow, corresponding with the red appearance of red corals.

3.2.4. Coral color comparison of the same pigment concentration

Since there is a large error in calculating the relative concentration of organic matter in red coral, after longitudinal stretching of the Raman spectrum, we picked up five groups of samples with the same inorganic signal intensity from the organic signal at $\nu(1,127\text{ cm}^{-1})$, $\nu(1,518\text{ cm}^{-1})$, and $\nu(1,088\text{ cm}^{-1})$ to study and discuss. After the stretching, the organic signal and inorganic signal intensity are the same, which means, the organic–inorganic signal intensity ratio is the same, the concentration of the organic energy group contained in the sample is the same, and the pigment concentration is the same.

As shown in Fig. 8 and Table 3, comparing samples of the same pigment concentration, we can find the following rules:

At the same pigment concentration, the lightness L^* of *Corallium elatius* and *Corallium rubrum* corals were similar, which were significantly higher than *Corallium japonicum* corals and corals of unknown species. This is due to the fact that *Corallium elatius* and *Corallium rubrum* corals contain more colorless and opaque organic small particles, such as sugars, lipids, proteins, etc. [13]. Although they have no color, they can significantly improve the lightness of the coral L^*

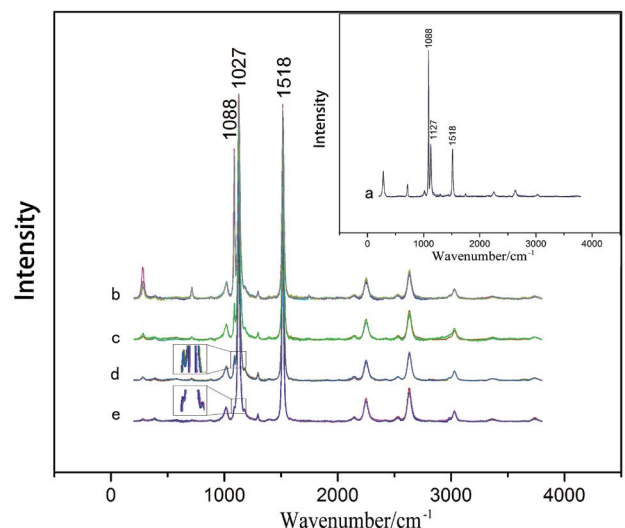
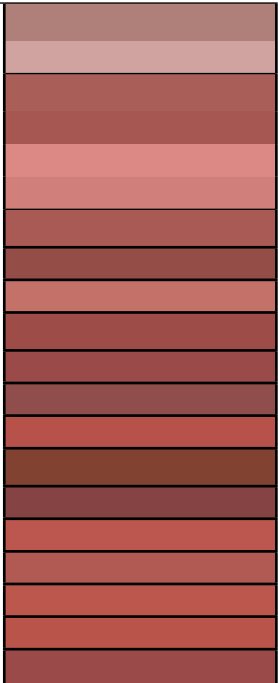


Fig. 8. Raman spectrum of red coral with the same pigment concentration.

Note: (a) Raman spectra of samples 08, M3, (b) Raman spectra of samples 10, 11, M8, and M9, (c) Raman spectra of samples No. 12, 13, and M11, (d) Raman spectra of samples A1, A2, A4, and M17, and (e) Raman spectra of samples A18, A20, M14, M16, S1, S4, and S7.

Table 3
Color data of five groups of samples a, b, c, d, e

Group	No	L*	a*	b*	C*	h_0	Simulation of color piece
a	08	58.11	18.3	11.32	21.51	31.74	
	M3	71.35	17.06	7.59	18.67	23.98	
	10	48.93	30.47	17.79	35.28	30.27	
b	11	46.72	32.6	18.93	37.69	30.14	
	M8	66.31	32.18	15.89	35.89	26.28	
	M9	62.22	32.36	16.68	36.41	27.27	
c	12	47.97	32.84	18.76	37.82	29.74	
	13	42.46	29.52	17.51	34.32	30.67	
	M11	57.29	32.93	19.47	38.26	30.59	
d	A1	43.23	34.11	19.71	39.39	30.02	
	A2	41.66	34.32	18.27	38.88	28.03	
	A4	40.75	28.05	14.33	31.49	27.06	
	M17	48.43	40.85	25.37	48.09	31.84	
	A18	35.67	27.01	12.79	29.88	25.34	
	A20	38.66	28.99	13.35	31.92	24.73	
e	M14	49.5	41.17	24.6	47.96	30.89	
	M16	48.78	35.03	21.3	40.99	31.3	
	S1	50.35	40.73	26.2	48.43	32.75	
	S4	48.76	40.68	25.86	48.2	32.44	
	S7	42.05	34.21	18.14	38.72	27.93	

and reduce its transparency, which is corresponding with the “porcelain texture” of *Corallium elatius* coral, the “Gummy texture” of *Corallium rubrum* coral, and “glass texture” of *Corallium japonicum* coral. In the future research, the brightness L^* and pigment concentration data of different species of red corals will be continuously enriched, and a database will be produced. Simply obtain the Raman spectrum and the lightness L^* of the red coral, and compare the databases, the species can be distinguished, which is a brand-new and non-destructive method for identifying coral species.

4. Conclusions

In the experiment, we used Raman spectroscopy and hand-held colorimeter to study the different species of red corals. The results show that the coral samples used in the study were all calcite instead of aragonite. The signal intensity ratio of Raman $\nu(715\text{ cm}^{-1})$ and $\nu(1,019\text{ cm}^{-1})$ in calcite was not constant, which is about angle between the testing laser and coral growth direction. Red coral is an organic calcite aggregate gemstone, so the tiny calcite crystals inside it are collectively oriented. The red coral of different biological species has the same Raman spectrum of the coloring organic pigment, which can be inferred that the color-developing pigments are the same. There is a positive correlation between the relative intensity of the main organic signals in the Raman spectrum, that is, the number of organic functional groups producing the signal is positively correlated, moreover, the Elson correlation coefficient is bigger than 0.95, indicating that the number of CH_2 , $\text{C}-\text{C}$, and $\text{C}=\text{C}$ functional groups in the polyene organic pigment is positively correlated. Under the standard D_{65} light

source, the color of the red coral sample is white-red, hue angle $h_0 \in (21.07, 151.98)$; the lightness is medium to upper, the lightness value L^* is (32.97, 88.70); the chroma's changing interval is large, chroma C^* is between (1.40, 48.42); after removing five white red corals without organic pigment, the red coral color is in the orange-red area, and the hue angle is $h_0 \in (21.07, 51.23)$. Such a large range of hue angles indicates that the pigmentation color of the coral is not single and the color is different, at least one color is red, and at least one color is orange-yellow, whose ratio and concentration change causes various colors of coral change.

Combining the results of previous studies [22,26], we hypothesized that the polyene pigment in coral is not a single one, but is a mixture of two polyene pigments, which are cis-trans isomers and polyenes. The length of the chain and the type of the functional group are the same. One color of the pigment is red, the hue angle h_0 is about 20 degrees, and the other pigment color is yellow-orange, and the hue angle $h_0 > 50$ degrees. Red coral also contains some colorless and opaque substances. This colorless opaque substance is a mixture of sugars, lipids, and proteins that affect the lightness L^* and transparency of corals. Moreover, the content of these colorless and opaque substances is related to the biological species of corals, and further enriching the specimen and establishing database in the future, which can be used as a non-destructive method for distinguishing coral species.

Acknowledgments

Completing this thesis, the author would like to express my great gratitude to those who have helped me a lot in the

research. Besides, the author also appreciate all the professors and teachers at the Laboratory of School of Gemology, China University of Geosciences (Beijing) for strong support for the colorimetry and spectroscopy experiments. Our great thanks are also to Anxin's great help in graphic design.

References

- [1] C.P. Smith, S. McClure, S. Eaton-Magana, D.M. Kondo, Pink-to-red coral: a guide to determining origin of color, *Gems Gemology*, 43 (2007) 4–15.
- [2] M.A. Ashraf, M.M. Hanafiah, Sustaining life on earth system through clean air, pure water, and fertile soil, *Environ. Sci. Pollut. Res.*, 26 (2019) 13679–13680.
- [3] J. Khan, S. Ilyas, B. Akram, M. Siddiq, M.A. Ashraf, Zn/NiO coated multi-walled carbon nanotubes for textile dyes degradation, *Arabian J. Chem.*, 11 (2018) 880–896.
- [4] J.A.J.M. Van de Water, C.R. Voolstra, C. Rottier, S. Cocito, A. Peirano, D. Allemand, C. Ferrier-Pages, Seasonal stability in the microbiomes of temperate gorgonians and the red coral *Corallium rubrum* across the Mediterranean Sea, *Microb. Ecol.*, 75 (2017) 274–288.
- [5] O.S. Onwuka, C.K. Ezugwu, S.I. Ifediegwu, Assessment of the impact of onsite sanitary sewage system and agricultural wastes on groundwater quality in Ikem and its environs, south-eastern Nigeria, *Geol. Ecol. Landscapes*, 3 (2019) 65–81.
- [6] L.I. Nodseth, Corals, blood and precious pearls: the materiality of a late medieval textile, *J. Art History*, 86 (2017) 173–187.
- [7] K. Uda, Y. Komeda, H. Koyama, K. Koga, T. Fujita, N. Iwasaki, T. Suzuki, Complete mitochondrial genomes of two Japanese precious corals, *Paracorallium japonicum* and *Corallium konojoi* (Cnidaria, Octocorallia, Coralliidae): notable differences in gene arrangement, *Gene*, 476 (2011) 27–37.
- [8] S. Qian, The damping loss prevention research on aerobics special shoe materials based on intelligent analysis, *Sci. Heritage J.*, 3 (2019) 20–23.
- [9] Y. Urushihara, H. Hasegawa, N. Iwasaki, X-ray micro-CT observation of the apical skeleton of Japanese white coral *Corallium konojoi*, *J. Exp. Mar. Biol. Ecol.*, 475 (2016) 124–128.
- [10] Y. Tamenori, T. Yoshimura, N.T. Luan, H. Hasegawa, A. Suzuki, H. Kawahata, N. Iwasaki, Identification of the chemical form of sulfur compounds in the Japanese pink coral (*Corallium elatius*) skeleton using μ -XRF/XAS speciation mapping, *J. Struct. Biol.*, 186 (2014) 214–223.
- [11] P. Abbas, Y.Z.H.Y. Hashim, H.M. Salleh, Cytotoxic effects and response surface optimization of solvent extraction of crude extracts from *Aquilaria subintegra* uninfected branch, *Sci. Heritage J.*, 2 (2018) 10–15.
- [12] R.G. Waller, A.R. Baco, Reproductive morphology of three species of deep-water precious corals from the Hawaiian archipelago: *gerardia* sp. *Corallium Secundum*, and *Corallium Lauuense*, *Bull. Mar. Sci.*, 81 (2007) 533–542.
- [13] A. Haguenaue, F. Zuberer, J.B. Ledoux, D. Aurelle, Adaptive abilities of the Mediterranean red coral *Corallium rubrum* in a heterogeneous and changing environment: from population to functional genetics, *J. Exp. Mar. Biol. Ecol.*, 449 (2013) 349–357.
- [14] I. Sufiyan, J.I. Magaji, Modeling flood hazard using SWAT and 3D analysis in Terengganu watershed, *J. CleanWas*, 2 (2018) 19–24.
- [15] R. Cannas, F. Sacco, A. Cau, D. Cuccu, M.C. Follesa, A. Cau, Genetic monitoring of deep-water exploited banks of the precious sardinia coral *Corallium rubrum* (L. 1758): useful data for a sustainable management, *Aquat. Conserv. Mar. Freshwater Ecosyst.*, 26 (2014) 236–250.
- [16] M. Pratlong, A. Haguenaue, S. Chenesseau, K. Brener, G. Mitta, E. Toulza, M. Bonabaud, S. Rialle, D. Aurelle, P. Pontarotti, Evidence for a genetic sex determination in cnidaria, the mediterranean red coral (*Corallium rubrum*), *R. Soc. Open Sci.*, 4 (2017) 1–9.
- [17] J. Ali, A.A.J. Mohamed, M.S.A. Kumar, B.A. John, Organophosphorus pesticides toxicity on brine shrimp, *Artemia*, *J. CleanWAS*, 2 (2018) 23–26.
- [18] J. Boavida, D. Paulo, D. Aurelle, S. Arnaud-Haond, C. Marschal, J. Reed, J.M.S. Gonçalves, E.A. Serrão, A well-kept treasure at depth: precious red coral rediscovered in Atlantic deep coral gardens (SW Portugal) after 300 years, *PLoS One*, 11 (2016) 1–26.
- [19] J.C. Merlin, M.L. Delé-Dubois, Resonance Raman characterization of polyacetylenic pigments in the calcareous skeleton, *Comp. Biochem. Physiol.*, 84B (1986) 97–103.
- [20] G. Ranson, A. Durivault, Le pigment d' *Heliopora coerulea* et de quelques autres alcyonnaires, *C R Soc. Biol. Paris*, 126 (1937) 1149–1151.
- [21] D. Allemand, M.C. Grillo, Biocalcification mechanism in gorgonians: ^{45}Ca uptake and deposition by the Mediterranean red coral *Corallium rubrum*, *J. Exp. Zool.*, 262 (1992) 237–246.
- [22] N.F.A. Rozuki, M.H. Tajuddin, N. Yusof, Effect of different solvent on asymmetric polysulfone (Psf) membranes for CO_2/CH_4 separation, *Environ. Ecosyst. Sci.*, 2 (2018) 11–14.
- [23] R.W. Grigg, Future prospects for coral reef science and species beyond the reef, *Coral Reefs*, 12 (1993) 55–56.
- [24] S. Laraib, S. Zulfiqar, N. Tabassum, S. Mukhtar, Current practices and efficacy of improvements in radioactive management system of Pakistan – a review, *Environ. Contam. Rev.*, 1 (2018) 09–12.
- [25] D. Vullo, D. Zoccola, S. Tambutté, C.T. Supuran, Activation profile analysis of *cruca4*, an alpha-carbonic anhydrase involved in skeleton formation of the mediterranean red coral, *Corallium rubrum*, *Molecules*, 23 (2017) 1–10.
- [26] Q. Ain, G. Rehman, M. Zaheer, An analysis of an underground water flow using Adomian decomposition method, *Water Conserv. Manage.*, 3 (2019) 27–29.
- [27] B. Kaczorowska, A. Hacura, T. Kupka, R. Wrzalik, E. Talik, G. Pasterny, A. Matuszewsk, Spectroscopic characterization of natural corals, *Anal. Bioanal. Chem.*, 377 (2003) 1032–1037.
- [28] L. Bergamonti, D. Bersani, S. Mantovan, P.P. Lottici, Micro-raman investigation of pigments and carbonate phases in corals and molluscan shells, *Eur. J. Mineral.*, 25 (2013) 845–853.
- [29] M.H. Mahtab, M. Ohara, M. Rasmy, The impact of rainfall variations on flash flooding in Haor Areas in Bangladesh, *Water Conserv. Manage.*, 2 (2018) 6–10.
- [30] S. Karampelas, E. Fritsch, J.Y. Mevellec, J.P. Gauthier, S. Sklavounos, T. Soldatos, Determination by raman scattering of the nature of pigments in cultured freshwater pearls from the mollusk *Hyriopsis cumingi*, *J. Raman Spectrosc.*, 38 (2007) 217–230.
- [31] J.C. Merlin, Resonance Raman spectroscopy of carotenoids and carotenoid-containing systems, *Pure Appl. Chem.*, 57 (1985) 785–792.
- [32] T. Kupka, H.R. Lin, L. Stobinski, C.H. Chen, W.J. Liou, R. Wrzalik, Z. Flisaka, Experimental and theoretical studies on corals. I. Toward understanding the origin of color in precious red corals from Raman and IR spectroscopies and DFT calculations, *J. Raman Spectrosc.*, 41 (2010) 651–658.
- [33] J. Cvejic, S. Tambutté, S. Lotto, M. Mikov, I. Slacanin, D. Allemand, Determination of canthaxanthin in the red coral (*Corallium rubrum*) from Marseille by HPLC combined with UV and MS detection, *Mar. Biol.*, 152 (2007) 855–862.
- [34] E. Fritsch, S. Karampelas, Comment on: determination of canthaxanthin in the red coral (*Corallium rubrum*) from Marseille by HPLC combined with UV and MS detection, *Mar. Biol.*, 154 (2008) 929–930.
- [35] S. Karampelas, E. Fritsch, J.Y. Mevellec, S. Sklavounos, T. Soldatos, Role of polyenes in the coloration of cultured freshwater pearls, *Eur. J. Mineral.*, 21 (2009) 85–97.
- [36] R.F. Fernandes, L.F. Maia, M.R.C. Couri, L.A.S. Costa, L.F.C. De Oliveira, Raman spectroscopy as a tool in differentiating conjugated polyenes from synthetic and natural sources, *Spectrochim. Acta, Part A*, 134 (2015) 434–441.
- [37] G. Galli, L. Bramanti, C. Priori, S. Rossi, G. Santangelo, G. Tsounis, C. Solidoro, Modelling red coral (*Corallium rubrum*) growth in response to temperature and nutrition, *Ecol. Modell.*, 337 (2016) 137–148.
- [38] R. Shamey, M.G. Sedito, R.G. Kuehni, Comparison of unique hue stimuli determined by two different methods using Munsell color chips, *Color Res. Appl.*, 35 (2010) 419–424.

- [39] R.R. George, The geochemistry of gems and its relevance to gemology: different traces, different prices, *Elements*, 5 (2009) 159–162.
- [40] S.C. Matz, R.J.P. De Figueiredo, A nonlinear image contrast sharpening approach based on Munsell's scale, *IEEE Trans. Image Process.*, 15 (2006) 900–909.
- [41] H.S. Cha, Y.K. Lee, Difference in illuminant-dependent color changes of shade guide tabs by the shade designation relative to three illuminants, *Am. J. Dent.*, 22 (2009) 350–356.
- [42] Y. Guo, Quality evaluation of tourmaline red based on uniform color space, *Cluster Comput.*, 20 (2017) 3393–3408.
- [43] Y. Guo, X. Zong, M. Qi, Feasibility study on quality evaluation of jadeite-jade color green based on gem dialogue color chip, *Multimedia Tools Appl.*, 78 (2019) 841–856.
- [44] Y. Guo, Quality grading system of jadeite-Jade green based on three colorimetric parameters under CIE standard light sources D65, CWF and A, *Bulg. Chem. Commun.*, 49 (2017) 961–968.
- [45] Y. Guo, H. Wang, X. Li, S.R. Dong, Metamerism appreciation of jadeite-Jade green under the standard light sources D65, A and CWF, *Acta Geol. Sin.*, 90 (2016) 2097–2103.
- [46] Y. Guo, H. Wang, H. Du, The foundation of a color-chip evaluation system of jadeite-jade green with color difference control of medical device, *Multimedia Tools Appl.*, 75 (2016) 1–12.
- [47] Y. Guo, X. Zhang, X. Li, Z. Ye, Quantitative characterization appreciation of golden citrine golden by the irradiation of $[\text{FeO}_4]^{4-}$, *Arabian J. Chem.*, 11 (2018) 918–923.
- [48] J. Urmos, S.K. Sharma, F.T. Mackenzie, Characterization of some biogenic carbonates with Raman spectroscopy, *Am. Mineral.*, 76 (1991) 641–646.